

---

# Representation Learning with Statistical Independence to Mitigate Bias

---

Ehsan Adeli<sup>\*1,2</sup> Qingyu Zhao<sup>\*1</sup> Adolf Pfefferbaum<sup>1</sup> Edith V. Sullivan<sup>1</sup>  
 Li Fei-Fei<sup>2</sup> Juan Carlos Nieves<sup>2</sup> Kilian M. Pohl<sup>1</sup>

## Abstract

Presence of bias (in datasets or tasks) is inarguably one of the most critical challenges in machine learning applications that has alluded to pivotal debates in recent years. Such challenges range from spurious associations between variables in medical studies to the bias of race in gender or face recognition systems. Controlling for all types of biases in the dataset curation stage is cumbersome and sometimes impossible. The alternative is to use the available data and build models incorporating fair representation learning. In this paper, we propose such a model based on adversarial training with two competing objectives to learn features that have (1) maximum discriminative power with respect to the task and (2) minimal statistical mean dependence with the protected (bias) variable(s). Our approach does so by incorporating a new adversarial loss function that encourages a vanished correlation between the bias and the learned features. We apply our method to synthetic data, medical images (containing task bias), and a dataset for gender classification (containing dataset bias). Our results show that the learned features by our method not only result in superior prediction performance but also are unbiased. The code is available at <https://github.com/QingyuZhao/BR-Net/>.

## 1. Introduction

A central challenge in practically all machine learning applications is how to identify and mitigate the effects of the bias present in the study. Bias can be defined as one or a set of extraneous protected variables that distort the relationship between the input (independent) and output (dependent) variables and hence lead to erroneous conclusions (Pourhoseingholi et al., 2012). In a variety of applications ranging from disease prediction to face recognition, machine learn-

ing models are built to predict labels from images. Variables such as age, sex, and race may influence the training process if the distribution of image labels is skewed with respect to them. In these situations, the model may learn the influence of the bias instead of actual discriminative cues.

The two most prevalent types of biases are dataset bias (Salimi et al., 2019; Khosla et al., 2012) and task bias (Lee et al., 2019; Huang & Yates, 2012). *Dataset bias* is often introduced due to the lack of enough data points spanning the whole spectrum of variations with respect to one or a set of protected variables (*i.e.*, variables that define the bias). For example, a model that predicts gender from face images may have different recognition capabilities for different races with uneven sizes of training samples (Buolamwini & Gebru, 2018). *Task bias*, on the other hand, can be introduced by intrinsic protected variables defined within the task. For instance, in neuroimaging applications, demographic variables such as gender (Eichler et al., 1992) or age (Dobrowolska et al., 2019) can pose as crucial protected variables; *i.e.*, they affect both the input (*e.g.*, neuroimages) and output (*e.g.*, diagnosis) of a prediction model so that they likely introduce a distorted association. Both bias types pose serious challenges to learning algorithms.

With the rapid development of deep learning methods, Convolutional Neural Networks (CNN) are emerging as eminent ways of extracting representations (features) from imaging data. However, like other machine learning methods, CNNs are prone to capturing any bias present in the task or dataset. Recent work has focused on methods for understating causal effects of bias on databases (Salimi et al., 2019; Khademi & Honavar, 2020) or learning fair models (Li & Vasconcelos, 2019; Tommasi et al., 2017; Khosla et al., 2012; Salimi et al., 2019) with de-biased representations based on recent developments on invariant feature learning (Ganin et al., 2016; Bechavod & Ligett, 2017) and domain adversarial learning (Elazar & Goldberg, 2018; Sadeghi et al., 2019). These methods have shown great potential to remove dataset bias when the protected variables are dichotomous or categorical. However, their applications to handling task bias and continuous protected variables are still under-explored.

In this paper, we propose a representation learning scheme that learns features predictive of class labels with minimal

---

<sup>\*</sup>Equal contribution <sup>1</sup>Department of Psychiatry and Behavioral Sciences, Stanford School of Medicine, Stanford, CA <sup>2</sup>Department of Computer Science, Stanford University, Stanford, CA.

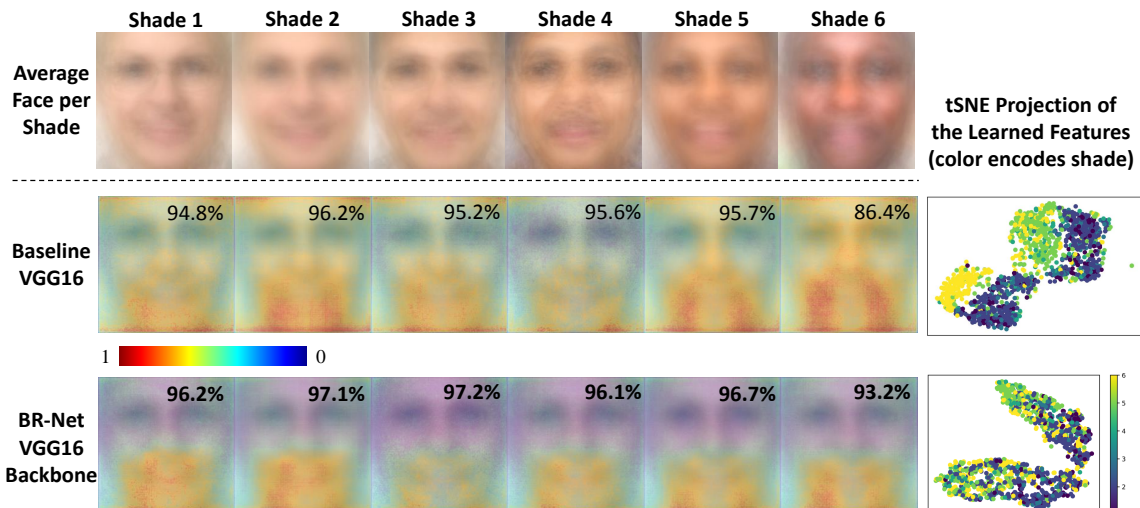


Figure 1. Average face images for each shade category (1<sup>st</sup> row), average saliency map of the trained baseline (2<sup>nd</sup> row), and BR-Net (3<sup>rd</sup> row) color-coded with the normalized saliency value for each pixel. BR-Net results in more stable patterns across all 6 shades. The last column shows the tSNE projection of the learned representations by each method. Our method results in a better representation space invariant to the bias variable (shade) while the baseline shows a clear pattern affected by the bias. Average accuracy of per-shade gender classification over 5 runs of 5-fold cross-validation (pre-trained on ImageNet, fine-tuned on GS-PPB) is shown on each average map. BR-Net is not only able to obtain better accuracy for the darker shade but it also regularizes the model to improve per-category accuracy.

bias to any generic type of protected variables. Our method is inspired by the domain-adversarial training approaches (Ganin et al., 2016) with controllable invariance (Xie et al., 2017) within the context of generative adversarial networks (GANs) (Goodfellow et al., 2014). We introduce an adversarial loss function based on the Pearson correlation between true and predicted values of a protected variable. Unlike prior methods, this strategy can handle protected variables that are continuous or ordinal. We theoretically show that the adversarial minimization of the linear correlation can remove non-linear association between the learned representations and protected variables, thus achieving *statistical mean independence*. Further, our strategy improves over the commonly used cross-entropy or mean-squared error (MSE) loss that only aim to predict the exact value of the bias variables and thereby achieves stabler results within the context of adversarial training. Since our proposed model injects resilience towards the bias during training to produce bias-invariant features, we refer to our approach as Bias-Resilient Neural Network (BR-Net). We apply our method to mitigate both dataset and task biases. BR-Net is different from the prior state-of-the-art fair representation learning methods as (1) it can deal with continuous protected variables and (2) is based on a theoretical proof of mean independence within the adversarial training context.

We evaluate BR-Net on three datasets that allow us to highlight different aspects of the method in comparison with a wide range of baselines. First, we test on a *synthetic dataset* to outline how the learned features by our method are unbiased to the protected variables. Then, we test it on a *medical imaging application*, *i.e.*, predicting the human immunode-

ficiency virus (HIV) diagnosis directly from T1-weighted Magnetic Resonance Images (MRIs). As documented by the HIV literature, HIV accelerates the aging process of the brain (Cole et al., 2017), thereby introducing a task bias with respect to age. In other words, if a predictor is trained not considering age as a protected variable (or confounder as referred to in medical studies), the predictor may actually learn the brain aging patterns rather than actual HIV markers. Lastly, we evaluate BR-Net for *gender classification* using the Gender Shades Pilot Parliaments Benchmark (GS-PPB) dataset (Buolamwini & Gebru, 2018). We use different backbones pre-trained on ImageNet (Deng et al., 2009) in BR-Net and fine-tune them for our specific task, *i.e.*, gender prediction from face images. We show that prediction accuracy of the vanilla model is dependent on the race of the subject (alternatively we consider skin color quantified by the ‘shade’ variable), which is not the case for BR-Net. Our comparison with several baselines and prior state-of-the-art shows that BR-Net is not only able to learn features impartial to race (verified by feature and saliency visualizations) but also results in higher classification accuracy (Fig. 1).

## 2. Related Work

**Fairness in Machine Learning:** In recent years, developing fair machine learning models have been the center of many discussions (Liu et al., 2018; Hashimoto et al., 2018; Barocas et al., 2017) including the media (Khullar, 2019; Miller, 2015). It is often argued that human or society biases are replicated in the training datasets and hence can be seen in learned models (Barocas & Selbst, 2016). Recent

effort in solving this problem focused on building fairer datasets (Yang et al., 2019; Celis et al., 2016; Salimi et al., 2019). However, this approach is not always practical for large-scale datasets or especially in medical applications, where data is relatively scarce and expensive to generate. To this end, other works learn fair representations leveraging the existing data (Zemel et al., 2013; Creager et al., 2019; Weinzaepfel & Rogez, 2019) by identifying features that are only predictive of the actual outputs, *i.e.*, impartial to the protected variable. However, prior work cannot be applied to continuous protected variables, which we address here.

**Domain-Adversarial Training:** (Ganin et al., 2016) proposed for the first time to use adversarial training for domain adaptation tasks by using the learned features to predict the domain label (a binary variable; source or target). Several other works built on top of the same idea and explored different loss functions (Bousmalis et al., 2017), domain discriminator settings (Tzeng et al., 2017; Edwards & Storkey, 2016; Beutel et al., 2017), or cycle-consistency (Hoffman et al., 2017). The focus of all these works was to close the domain gap, which is often encoded as a binary variable. To learn general-purpose bias-resilient models, we need to learn features invariant to all types of protected variables. Hence, we require new theoretical insight into the methods.

**Invariant Representation Learning:** There have been different attempts in the literature for learning representations that are invariant to specific factors in the data. For instance, (Zemel et al., 2013) took an information obfuscation approach to obfuscate membership in the protected group of data during training, and (Bechavod & Ligett, 2017; Ranzato et al., 2007) introduced regularization-based methods. Recently, (Xie et al., 2017; Akuzawa et al., 2019; Zhang et al., 2018; Elazar & Goldberg, 2018; Choi et al., 2019) proposed to use domain-adversarial training strategies for invariant feature learning. Some works (Sadeghi et al., 2019; Wang et al., 2019) used adversarial techniques based on similar loss functions as in domain adaptation to predict the exact values of the protected variables. For instance, (Wang et al., 2019) used a binary cross-entropy for removing effect of ‘gender’ and (Sadeghi et al., 2019) used linear and kernelized least-square predictors as the adversarial component. Several methods based on entropy (Springenberg, 2015; Roy & Boddeti, 2019) and mutual-information (Song et al., 2019; Bertran et al., 2019; Moyer et al., 2018) were also widely used for fair representation learning. However, these methods become intractable when protected variables are continuous or ordinal.

### 3. Bias-Resilient Neural Network (BR-Net)

Suppose we have an  $M$ -class classification problem, for which we have  $N$  pairs of training images and their corresponding target label(s):  $\{(\mathbf{X}_i, \mathbf{y}_i)\}_{i=1}^N$ . Assuming a set

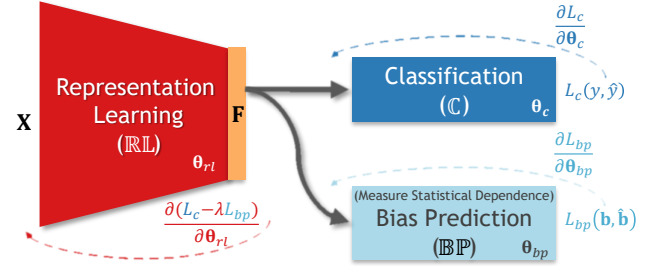


Figure 2. BR-Net architecture:  $\mathbb{R}\mathbb{L}$  learns features,  $\mathbf{F}$ , that successfully classify ( $\mathbb{C}$ ) the input while being invariant (not statistically dependent) to the protected variables,  $\mathbf{b}$ , using  $\mathbb{B}\mathbb{P}$  and the adversarial loss,  $-\lambda L_{bp}$  (based on correlation coefficient). Forward arrows show forward paths while the backward dashed ones indicate back-propagation with the respective gradient ( $\partial$ ) values.

of  $k$  protected variables, denoted by a vector  $\mathbf{b} \in \mathbb{R}^k$ , to train a model for classifying each image while being impartial to the protected variables, we propose an *end-to-end* architecture (Fig. 2) similar to domain-adversarial training approaches (Ganin et al., 2016). Given the input image  $\mathbf{X}$ , the representation learning ( $\mathbb{R}\mathbb{L}$ ) module extracts a feature vector  $\mathbf{F}$ , on top of which a Classifier ( $\mathbb{C}$ ) is built to predict the class label  $\mathbf{y}$ . Now, to guarantee that these features are not biased to  $\mathbf{b}$ , we build another network (denoted by  $\mathbb{B}\mathbb{P}$ ) with a new loss function that checks the statistical mean dependence of the protected variables to  $\mathbf{F}$ . Back-propagate this loss to the  $\mathbb{R}\mathbb{L}$  module in an adversarial way results in features that minimize the classification loss while having the least statistical dependence on the protected variables.

Each network has its underlying trainable parameters, defined as  $\theta_{rl}$  for  $\mathbb{R}\mathbb{L}$ ,  $\theta_c$  for  $\mathbb{C}$ , and  $\theta_{bp}$  for  $\mathbb{B}\mathbb{P}$ . If the predicted probability that subject  $i$  belongs to class  $m$  is defined by  $\hat{y}_{im} = \mathbb{C}(\mathbb{R}\mathbb{L}(\mathbf{X}_i; \theta_{rl}); \theta_c)$ , the classification loss can be characterized by a cross-entropy:

$$L_c(\mathbf{X}, \mathbf{y}; \theta_{rl}, \theta_c) = - \sum_{i=1}^N \sum_{m=1}^M y_{im} \log(\hat{y}_{im}). \quad (1)$$

Similarly, with  $\hat{\mathbf{b}}_i = \mathbb{B}\mathbb{P}(\mathbb{R}\mathbb{L}(\mathbf{X}_i; \theta_{rl}); \theta_{bp})$ , we can define the adversarial component of the loss function. Standard methods for designing this loss function suggest to use a cross-entropy for binary/categorical variables (*e.g.*, in (Ganin et al., 2016; Xie et al., 2017; Choi et al., 2019)) or an  $\ell_2$  MSE loss for continuous variables ((Sadeghi et al., 2019)). However, the ultimate goal of adversarial component is to remove statistical association with respect to the protected variables, as opposed to maximizing the prediction error of them. In fact, the adversarial training based on MSE leads to the maximization of the  $\ell_2$  distance between  $\hat{\mathbf{b}}$  and  $\mathbf{b}$ , which could be trivially achieved by uniformly shifting the magnitude of  $\hat{\mathbf{b}}$ , thereby potentially resulting in an ill-posed optimization and oscillation in the adversarial

training. To avoid this issue, we define the surrogate loss for predicting the protected variables while quantifying the statistical dependence with respect to  $\mathbf{b}$  based on the squared Pearson correlation  $\text{corr}^2(\cdot, \cdot)$ :

$$L_{bp}(\mathbf{X}, \mathbf{b}; \theta_{rl}, \theta_{bp}) = - \sum_{\kappa=1}^k \text{corr}^2(\mathbf{b}_{\kappa}, \hat{\mathbf{b}}_{\kappa}), \quad (2)$$

where  $\mathbf{b}_{\kappa}$  defines the vector of  $\kappa^{\text{th}}$  protected variable across all  $N$  training inputs. Through adversarial training, we aim to remove statistical dependence by encouraging a zero correlation between  $\mathbf{b}_{\kappa}$  and  $\hat{\mathbf{b}}_{\kappa}$ . Note,  $\mathbb{BP}$  deems to maximize squared correlation and  $\mathbb{RL}$  minimizes for it. Since  $\text{corr}^2$  is bounded in the range  $[0, 1]$ , both minimization and maximization schemes are feasible. Hence, the overall objective of the network is then defined as

$$\min_{\theta_{rl}, \theta_c} \max_{\theta_{bp}} L_c(\mathbf{X}, \mathbf{y}; \theta_{rl}, \theta_c) - \lambda L_{bp}(\mathbf{X}, \mathbf{b}; \theta_{rl}, \theta_{bp}). \quad (3)$$

where hyperparameter  $\lambda$  controls the trade-off between the two objectives. This scheme is similar to GAN (Goodfellow et al., 2014) and domain-adversarial training (Ganin et al., 2016; Xie et al., 2017), in which a min-max game is defined between two networks. In our case,  $\mathbb{RL}$  extracts features that minimize the classification criterion, while ‘fooling’  $\mathbb{BP}$  (i.e., making  $\mathbb{BP}$  incapable of predicting the protected variables). Hence, the saddle point for this objective is obtained when the parameters  $\theta_{rl}$  minimize the classification loss while maximizing the loss of  $\mathbb{BP}$ .

### 3.1. Non-linear Statistical Independence Guarantee

In general, a zero-correlation or a zero-covariance only quantifies linear independence between variables but cannot infer non-linear relationships. However, we now theoretically show that, under certain assumptions on the adversarial training of  $\mathbb{BP}$ , a zero-covariance would guarantee the *mean independence* (Wooldridge, 2010) between protected variables and the features, a much stronger type of statistical independence than the linear one.

A random variable  $\mathcal{B}$  is said to be *mean independent* of  $\mathcal{F}$  if and only if  $E[\mathcal{B}|\mathcal{F} = \xi] = E[\mathcal{B}]$  for all  $\xi$  with non-zero probability, where  $E[\cdot]$  defines the expected value. In other words, the expected value of  $\mathcal{B}$  is neither linearly nor non-linearly dependent on  $\mathcal{F}$ , but the variance of  $\mathcal{B}$  might. The following theorem then relates the mean independence between features  $\mathcal{F}$  and the protected variables  $\mathcal{B}$  to the zero-covariance between  $\mathcal{B}$  and the  $\mathbb{BP}$  prediction,  $\hat{\mathcal{B}}$ .

*Property 1:*  $\mathcal{B}$  is mean independent of  $\hat{\mathcal{B}} \Rightarrow \text{Cov}(\mathcal{B}, \hat{\mathcal{B}}) = 0$ .

*Property 2:*  $\mathcal{B}, \mathcal{F}$  are mean independent  $\Rightarrow \mathcal{B}$  is mean independent of  $\hat{\mathcal{B}} = \phi(\mathcal{F})$  for any mapping function  $\phi$ .

**Theorem 1.** Given random variables  $\mathcal{F}, \mathcal{B}, \hat{\mathcal{B}}$  with finite second moment,  $\mathcal{B}$  is mean independent of  $\mathcal{F} \Leftrightarrow$  for any arbitrary mapping  $\phi$ , s.t.  $\hat{\mathcal{B}} = \phi(\mathcal{F})$ ,  $\text{cov}(\mathcal{B}, \hat{\mathcal{B}}) = 0$

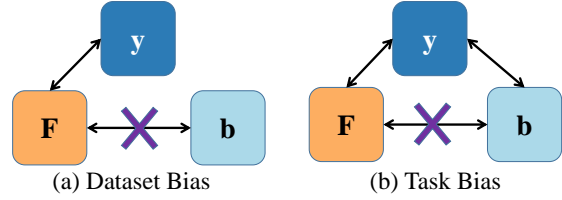


Figure 3. Dependency relations between variables for dataset or task bias. BR-Net removes direct dependency between  $\mathbf{F}$  and  $\mathbf{b}$ .

*Proof.* The forward direction  $\Rightarrow$  follows directly through *Property 1* and 2. We focus the proof on the reverse direction. Now, construct a mapping function  $\hat{\mathcal{B}} = \phi(\mathcal{F}) = E[\mathcal{B}|\mathcal{F}]$ , i.e.,  $\phi(\xi) = E[\mathcal{B}|\mathcal{F} = \xi]$ , then  $\text{Cov}(\mathcal{B}, \hat{\mathcal{B}}) = 0$  implies

$$E[\mathcal{B}E[\mathcal{B}|\mathcal{F}]] = E[\mathcal{B}]E[E[\mathcal{B}|\mathcal{F}]]. \quad (4)$$

Due to the self-adjointness of the mapping  $\mathcal{B} \mapsto E[\mathcal{B}|\mathcal{F}]$ , the left hand side of Eq. (4) reads  $E[\mathcal{B}E[\mathcal{B}|\mathcal{F}]] = E[(E[\mathcal{B}|\mathcal{F}])^2] = E[\hat{\mathcal{B}}^2]$ . By the law of total expectation  $E[E[\mathcal{B}|\mathcal{F}]] = E[\mathcal{B}]$ , the right hand side of Eq. (4) becomes  $E[\hat{\mathcal{B}}]^2$ . By Jensen’s (in)equality,  $E[\hat{\mathcal{B}}^2] = E[\hat{\mathcal{B}}]^2$  holds iff  $\hat{\mathcal{B}}$  is a constant, i.e.,  $\mathcal{B}$  is mean independent of  $\mathcal{F}$ .  $\square$

**Remark.** In practice, we normalize the covariance by standard deviations of variables for optimization stability. In the unlikely singular case that  $\mathbb{BP}$  outputs a constant, we add a small perturbation in computing the standard deviation.

This theorem echoes the validity of our adversarial training strategy:  $\mathbb{RL}$  encourages a zero-correlation between  $\mathbf{b}_{\kappa}$  and  $\hat{\mathbf{b}}_{\kappa}$ , which enforces  $\mathbf{b}_{\kappa}$  to be mean independent of  $\mathbf{F}$  (one cannot infer the expected value of  $\mathbf{b}_{\kappa}$  from  $\mathbf{F}$ ). In turn, assuming  $\mathbb{BP}$  has the capacity to approximate any arbitrary mapping function, the mean independence between features and bias would correspond to a zero-correlation between  $\mathbf{b}_{\kappa}$  and  $\hat{\mathbf{b}}_{\kappa}$ , otherwise  $\mathbb{BP}$  would adversarially optimize for a mapping function that increases the correlation.

Moreover, **Theorem 1** induces that when  $\mathbf{b}_{\kappa}$  is mean independent of  $\mathbf{F}$ ,  $\mathbf{b}_{\kappa}$  is also mean independent of  $\mathbf{y}$  for any arbitrary classifier  $\mathcal{C}$ , indicating that the prediction is guaranteed to be unbiased. When  $\mathcal{C}$  is a binary classifier and  $\mathbf{y} \sim \text{Ber}(q)$ , we have  $p(\mathbf{y} = 1|\mathbf{b}_{\kappa}) = E[\mathbf{y}|\mathbf{b}_{\kappa}] = E[\mathbf{y}] = p(\mathbf{y} = 1) = q$ ; that is,  $\mathbf{y}$  and  $\mathbf{b}_{\kappa}$  are fully independent.

### 3.2. Dataset vs. Task Bias

As mentioned, when  $\mathbf{b}$  characterizes dataset bias (Fig. 3a), there is no intrinsic link between the protected variable and the task label (e.g., in gender recognition, probability of being a female is not dependent on race), and the bias is introduced due to the data having a skewed distribution with respect to the protected variable. In this situation, we should train  $\mathbb{BP}$  on the entire dataset to remove dependency between  $\mathbf{F}$  and  $\mathbf{b}$ . On the other hand, when  $\mathbf{b}$  is a task bias

(Fig. 3b), it will have an intrinsic dependency with the task label (*e.g.*, in disease classification, the disease group has a different age range than the control group), such that the task label  $\mathbf{y}$  could potentially become a moderator (Baron & Kenny, 1986) that affects the strength of dependency between the features and protected variables. In this situation, the goal of fair representation learning is to remove the direct statistical dependency between  $\mathbf{F}$  and  $\mathbf{b}$  while tolerating the indirect association induced by the task. Therefore, our adversarial training aims to ensure mean independency between  $\mathbf{F}$  and  $\mathbf{b}$  conditioned on the task label

$$E[\mathbf{F}|\mathbf{b}, \mathbf{y}] = E[\mathbf{F}|\mathbf{y}], E[\mathbf{b}|\mathbf{F}, \mathbf{y}] = E[\mathbf{b}|\mathbf{y}]. \quad (5)$$

In practice, we achieve this objective by training an adversarial loss within one or each of the  $M$  classes, depending on the specific task.

### 3.3. Implementation Details

Similar to the training of GANs, in each iteration, we first back-propagate the  $L_c$  loss to update  $\theta_{rl}$  and  $\theta_c$ . With  $\theta_{rl}$  fixed, we then minimize the  $L_{bp}$  loss to update  $\theta_{bp}$ . Finally, with  $\theta_{bp}$  fixed, we maximize the  $L_{bp}$  loss to update  $\theta_{rl}$ . In this study,  $L_{bp}$  depends on the correlation operation, which is a population-based operation, as opposed to individual-level error metrics such as cross-entropy or MSE losses. Therefore, we calculate the correlations over each training batch as a batch-level operation. Depending on the application, we can use different architectures for each of the three subnetworks. We use a 3D CNN (Esmailzadeh et al., 2018; Nie et al., 2016) for  $\mathbb{R}L$  to extract features from 3D neuroimages and use VGG16 (Simonyan & Zisserman, 2015) and ResNet50 (He et al., 2015) backbones for GS-PPB. For  $\mathbb{C}$  and  $\mathbb{B}P$ , we use a two-layer fully connected network.

## 4. Experiments

In this section, we evaluate our method on three different scenarios. We compare BR-Net with several baseline approaches, and evaluate how our learned representations are invariant to the protected variables.

**Baseline Methods.** In line with the implementation of our approach, the baselines for all three experiments are 1) Vanilla: a vanilla CNN with an architecture exactly the same as BR-net without the bias prediction sub-network and hence the adversarial loss; and 2) Multi-task: a single  $\mathbb{R}L$  followed by two separate predictors for predicting  $\mathbf{b}_k$  and  $\mathbf{y}$ , respectively (Lu et al., 2017). The third type of approaches used for comparison are other unbiased representation learning methods. Note that most existing works for “fair deep learning” are only designed for categorical bias variables. Therefore, in the synthetic and brain MRI experiments where the protected variable is continuous, we compare with two applicable scenarios originally proposed

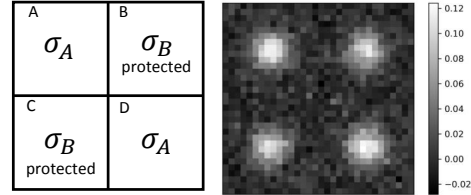


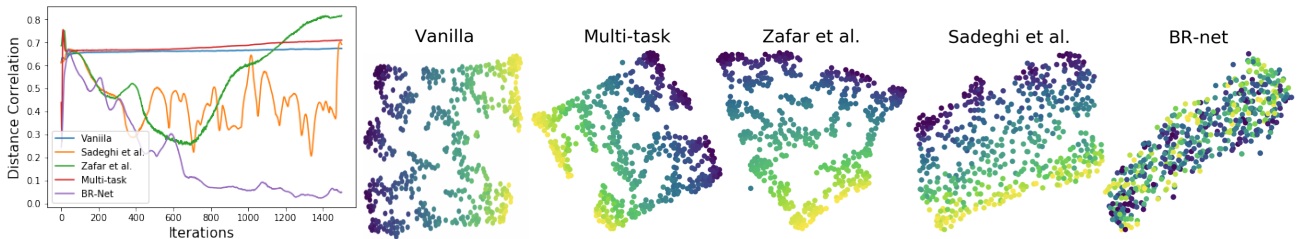
Figure 4. Synthetic data image synthesis.

in the logistic regression setting: 1) (Sadeghi et al., 2019) uses the MSE between the predicted and true bias as the adversarial loss; 2) (Zafar et al., 2017) aims to minimize the magnitude of correlation between  $\mathbf{b}_k$  and the logit of  $\mathbf{y}$ , which in our case is achieved by adding the correlation magnitude to the loss function. For the Gender Shades PPB experiment, the protected variable is categorical. We then further compare with (Kim et al., 2019), which uses conditional entropy as the adversarial loss to minimize the mutual information between bias and features. Note, entropy-based (Springenberg, 2015; Roy & Boddeti, 2019) and mutual-information-based methods (Song et al., 2019; Bertran et al., 2019; Moyer et al., 2018) are widely used in fair representation learning to handle discrete bias.

**Metrics for Accuracy and Statistical Independence.** For the MRI and GS-PPB experiments, we measure prediction accuracy of each method by recording the balanced accuracy (bAcc),  $F_1$ -score, and AUC from a 5-fold cross-validation. In addition, we measure the statistical dependency between the protected variable and features learned by each method. This is achieved by training the model on the entire dataset and then computing the squared distance correlation ( $dcor^2$ ) (Székely et al., 2007) and mutual information (MI) between the learned features and protected variable. Unlike Pearson correlation,  $dcor^2 = 0$  or  $MI = 0$  imply full statistical independence between variables. Even though the MI between high-dimensional features and continuous protected variables is intractable to optimize during training, it still can be approximated in the validation stage. Lastly, the discrete protected variable in GS-PPB experiment allows us to record another independence metric called the Equality of Opportunity (EO). EO measures the average gap in true positive rates w.r.t. different values of the protected variable.

### 4.1. Synthetic Data

We generate a synthetic dataset comprised of two groups of data, each containing 512 images of resolution  $32 \times 32$  pixels. Each image is generated by 4 Gaussians (see Fig. 4), the magnitude of which is controlled by  $\sigma_A$  and  $\sigma_B$ . For each image from Group 1, we sample  $\sigma_A$  and  $\sigma_B$  from a uniform distribution  $\mathcal{U}(1, 4)$  while we generate images of Group 2 with stronger intensities by sampling from  $\mathcal{U}(3, 6)$ . Gaussian noise is added to the images with standard deviation 0.01. Now we assume the difference



(a) Distance correlation w.r.t.  $\sigma_B$  (b) tSNE projection of the learned features for different methods. Color indicates the value of  $\sigma_B$ .  
Figure 5. Comparison of results on the synthetic dataset.

in  $\sigma_A$  between the two groups is associated with the true discriminative cues that should be learned by a classifier, whereas  $\sigma_B$  is a protected variable. In other words, an unbiased model should predict the group label purely based on the two diagonal Gaussians and not dependent on the two off-diagonal ones. To show that the BR-Net can result in such models by controlling for  $\sigma_B$ , we train it on the whole dataset of 1,024 images with binary labels and  $\sigma_B$  values.

For simplicity, we construct  $\mathbb{R}\mathbb{L}$  with 3 stacks of  $2 \times 2$  convolution/ReLU/max-pooling layers to produce 32 features. Both the  $\mathbb{B}\mathbb{P}$  and  $\mathbb{C}$  networks have one hidden layer of dimension 16 with  $\tanh$  as the non-linear activation function. After training, the vanilla and multi-task models achieve close to 95% training accuracy, and the other 3 methods close to 90%. Note that the theoretically maximum training accuracy is 90% due to the overlapping sampling range of  $\sigma_A$  between the two groups, indicating that the vanilla and multi-task models additionally rely on the protected variable  $\sigma_B$  for predicting the group label, an undesired behavior. Further, Fig. 5a shows that our method can optimally remove the statistical association w.r.t.  $\sigma_B$  as  $dcor^2$  drops dramatically with training iterations. The MSE-based adversarial loss yields unstable  $dcor^2$  measures potentially due to the ill-posed optimization of maximizing  $\ell_2$  distance. Moreover, minimizing the statistical association between the bias and predicted label  $y$  (Zafar et al., 2017) does not necessarily lead to unbiased features (green curve Fig. 5a). Finally, the above results are further supported by the 2D t-SNE (Maaten & Hinton, 2008) projection of the learned features as shown in Fig. 5b. BR-net results in a feature space with no apparent bias, whereas features derived by other methods form a clear correlation with  $\sigma_B$ . This confirms the unbiased representation learned by BR-Net.

## 4.2. HIV Diagnosis Based on MRIs

Our second task aims at diagnosing HIV patients *vs.* control subjects (CTRL) based on brain MRIs. The study cohort includes 223 CTRLs and 122 HIV patients who are seropositive for the HIV-infection with CD4 count  $> 100 \frac{\text{cells}}{\mu\text{L}}$  (average: 303.0). Since the HIV subjects are significantly older in age than the CTRLs (CTRL:  $45 \pm 17$ , HIV:  $51 \pm 8.3$ ,

Table 1. Classification accuracy of HIV diagnosis prediction and statistical dependency of learned features w.r.t. age. Best result in each column is typeset in bold and the second best is underlined.

Method	bAcc	F <sub>1</sub>	AUC	$dcor^2$	MI
Vanilla	71.8	0.64	80.8	0.21	0.07
Multi-task	<b>74.2</b>	<u>0.66</u>	<b>82.5</b>	0.47	1.31
(Sadeghi et al., 2019)	64.8	0.58	75.2	0.22	0.06
(Zafar et al., 2017)	<u>73.2</u>	0.65	80.8	<u>0.15</u>	<u>0.04</u>
BR-Net (Ours)	<b>74.2</b>	<b>0.67</b>	<u>80.9</u>	<b>0.05</b>	<b>7e-4</b>

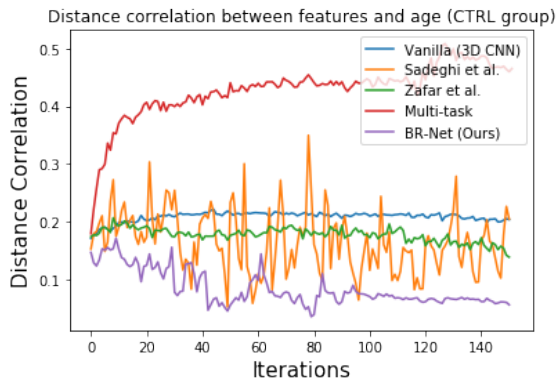


Figure 6. Distance correlation between the learned features and age for the CTRL cohort in the HIV experiment.

$p < .001$ ) in this study, normal aging becomes a potential task bias; prediction of diagnosis labels may be dependent on subjects' age instead of true HIV markers.

The T1-weighted MRIs are all skull stripped, affinely registered to a common template, and resized into a  $64 \times 64 \times 64$  volume. For each run of the 5-fold cross-validation, the training folds are augmented by random shifting (within one-voxel distance), rotation (within one degree) in all 3 directions, and left-right flipping based on the assumption that HIV infection affects the brain bilaterally (Adeli et al., 2018). The data augmentation results in a balanced training set of 1024 CTRLs and 1024 HIVs. As the flipping removes left-right orientation, the ConvNet is built on half of the 3D volume containing one hemisphere. The representation extractor  $\mathbb{R}\mathbb{L}$  has 4 stacks of  $2 \times 2 \times 2$  3D convolution/ReLU/batch-normalization/max-pooling layers

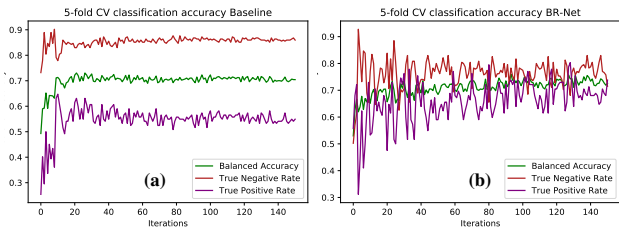


Figure 7. Accuracy, true negative, and true positive rates of the HIV experiment, as a function of the # of iterations for (a) vanilla 3D CNN baseline, (b) BR-Net. The results show that our method is robust against the imbalanced age distribution between HIV and CTRL subjects and achieves balanced prediction for both cohorts.

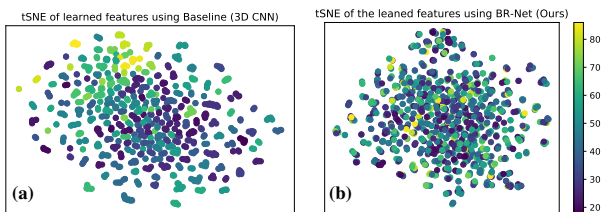


Figure 8. tSNE visualization of the learned features by (a) the 3D CNN baseline and (b) our BR-Net. Each point shows a subject in the CTRL cohort color-coded by their age.

yielding 4096 intermediate features. Both  $\mathbb{B}P$  and  $\mathbb{C}$  have one hidden layer of dimension 128 with  $\tanh$  as the activation function. As discussed, the task bias should be handled within individual groups rather the whole dataset. Motivated by recent medical studies (Rao et al., 2017; Adeli et al., 2018), we perform the adversarial training with respect to the protected variable of age only on the CTRL group because HIV subjects may exhibit irregular aging. This practice ensures that the features of both CTRL and HIV subjects are unbiased towards normal aging.

Table 1 shows the diagnosis prediction accuracy of BR-Net in comparison with baseline methods. BR-Net results in the most accurate prediction in terms of balanced accuracy (bAcc) and  $F_1$ -score, while it also learns the least biased features in terms of  $dcor^2$  and MI. While the multi-task model produces a higher AUC, it is also the most biased model as it learns features with highest dependency w.r.t. age. This result is also supported by Fig. 6, where the distance cor-

relation for BR-Net decreases with the adversarial training and increases for Multi-task. Similar to the synthetic experiment, adversarial training based on MSE-loss produces inconsistent and unreliable associations with age. The t-SNE projections of the learned feature spaces are visualized in Fig. 8. The feature space learned by the vanilla model forms a clear association with age, as older subjects are concentrated on the top left region of the space. This again suggests predictions from the baseline may be dependent on age rather than true HIV markers. Whereas, our method results in a space with no apparent bias to age. In addition, we record the true positive and true negative rate of BR-net for each training iteration. As shown in Fig. 7, the baseline tends to predict most subjects as CTRLs (high true negative rate). This is potentially caused by the CTRL group having a wider age distribution, so an age-dependent predictor would bias the prediction towards CTRL. When controlling age as a protected variable, BR-Net reliably results in balanced true positive and true negative rates.

### 4.3. Gender Prediction Using the GS-PPB Dataset

The last experiment is on gender prediction from face images in the Gender Shades Pilot Parliaments Benchmark (GS-PPB) dataset (Buolamwini & Gebru, 2018). This dataset contains 1,253 facial images of 561 female and 692 male subjects. The face shade is quantified by the Fitzpatrick six-point labeling system and is categorised from type 1 (lighter) to type 6 (darker). This quantization was used by dermatologists for skin classification and determining risk for skin cancer (Buolamwini & Gebru, 2018). To ensure prediction is purely based on facial areas, we first perform face detection and crop the images (Geitgey, 2018).

To train our models on this dataset, we use backbones VGG16 (Simonyan & Zisserman, 2015) and ResNet50 (He et al., 2015) pre-trained on ImageNet (Deng et al., 2009). We fine-tune each model on GS-PPB dataset to predict the gender of subjects based on their face images using fair 5-fold cross-validation. The ImageNet dataset for pre-training the models has fewer cases of humans with darker faces (Yang et al., 2019), and hence the resulting models have an underlying dataset bias to the shade.

BR-Net counts the variable ‘shade’ as an ordinal and cat-

Table 2. Average prediction results over five runs of 5-fold cross-validation and statistical independence metrics derived on the GS-PPB dataset. Best results in each column are typeset in bold and second best are underlined.

Method	VGG16 Backbone						ResNet50 Backbone					
	bAcc (%)	$F_1$ (%)	AUC (%)	$dcor^2$	MI	EO%	bAcc (%)	$F_1$ (%)	AUC (%)	$dcor^2$	MI	EO%
Vanilla	94.1±0.2	93.5±0.3	98.9±0.1	0.17	0.40	4.29	75.7±2.0	68.0±3.0	96.2±0.3	0.29	0.60	11.2
(Kim et al., 2019)	95.8±0.5	95.7±0.5	99.2±0.2	0.32	0.28	4.12	91.4±0.9	91.0±0.9	96.6±0.7	<b>0.18</b>	0.55	3.86
(Zafar et al., 2017)	94.3±0.4	93.7±0.5	99.0±0.1	0.19	0.43	4.11	<b>94.2±0.4</b>	<b>93.6±0.4</b>	<b>98.7±0.1</b>	0.29	0.60	4.68
Multi-Task	94.0±0.3	93.4±0.3	98.9±0.1	0.28	0.42	4.45	94.0±0.3	93.4±0.3	98.6±0.3	0.29	0.63	4.15
BR-Net	<b>96.3±0.6</b>	<b>96.0±0.7</b>	<b>99.4±0.2</b>	<b>0.12</b>	<b>0.13</b>	<b>2.02</b>	94.1±0.2	<b>93.6±0.2</b>	<u>98.6±0.1</u>	0.23	<b>0.49</b>	<b>2.87</b>

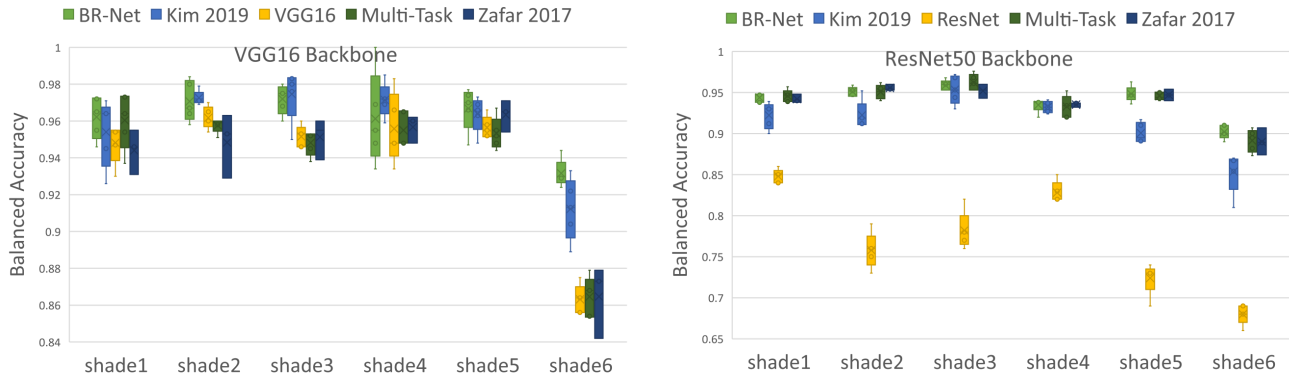


Figure 9. Accuracy of gender prediction from face images across all shades (1 to 6) of the GS-PPB dataset with two backbones, (left) VGG16 and (right) ResNet50. BR-Net consistently results in more accurate predictions in all 6 shade categories.

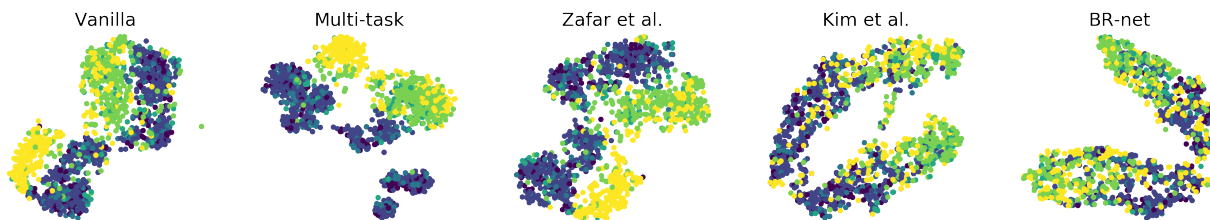


Figure 10. Learned representations by different methods. Color encodes the 6 categories of skin shade.

egorical protected variable. As discussed earlier, besides the baseline models in the HIV experiment, we additionally compare with a fair representation learning method, (Kim et al., 2019), based on mutual information minimization. Note that this method is designed to handle discrete protected variables, therefore not applicable in previous experiments. We exclude (Sadeghi et al., 2019) as the adversarial MSE-loss results in large oscillation in prediction results. Table 2 shows the prediction results across five runs of 5-fold cross-validation and the independence metrics derived by training on the entire dataset. Fig. 9 plots the accuracy for each individual ‘shade’ category. In terms of bAcc, BR-Net results in more accurate gender prediction than all baseline methods except that it is slightly worse than (Zafar et al., 2017) with ResNet50 backbone. However, features learned by (Zafar et al., 2017) are more biased towards skin shade. In most cases our method produces less biased features than (Kim et al., 2019), a method designed to explicitly optimize full statistical independence between variables. In practice, removing mean dependency by adversarial training is potentially a better surrogate for removing statistical dependency between high-dimensional features and bias.

BR-Net produces similar accuracy across all ‘shade’ categories. Prediction made by other methods, however, is more dependent on the protected variable by showing inconsistent recognition capabilities for different ‘shade’ categories and failing significantly on darker faces. This bias is confirmed by the t-SNE projection of the feature spaces (see

Fig. 10) learned by the baseline methods; they all form clearer association with the bias variable than BR-Net. To gain more insight, we visualize the saliency maps derived for the baseline and BR-Net. For this purpose, we use a similar technique as in (Simonyan et al., 2014) to extract the pixels in the original image space highlighting the areas that are discriminative for the gender labels. Generating such saliency maps for all inputs, we visualize the average map for each individual ‘shade’ category (Fig. 1). The value on each pixel corresponds to the attention from the network to that pixel within the classification process. Compared to the baseline, BR-Net focuses more on specific face regions and results in more stable patterns across all ‘shade’ categories.

## 5. Conclusion

Machine learning models are acceding to everyday lives from policy making to crucial medical applications. Failure to account for the underlying bias in datasets and tasks can lead to spurious associations and erroneous decisions. We proposed a method based on adversarial training strategies by encouraging vanished correlation to learn features for the prediction task while being unbiased to the protected variables in the study. We evaluated our bias-resilient neural network (BR-Net) on synthetic, medical diagnosis, and gender classification datasets. In all experiments, BR-Net resulted in representations that were invariant to the protected variable while obtaining comparable (and sometime better) classification accuracy.



## References

- Adeli, E., Kwon, D., Zhao, Q., Pfefferbaum, A., Zahr, N. M., Sullivan, E. V., and Pohl, K. M. Chained regularization for identifying brain patterns specific to HIV infection. *NeuroImage*, 183:425–437, 2018.
- Akuzawa, K., Iwasawa, Y., and Matsuo, Y. Adversarial invariant feature learning with accuracy constraint for domain generalization. *arXiv preprint arXiv:1904.12543*, 2019.
- Barocas, S. and Selbst, A. D. Big data’s disparate impact. *Calif. L. Rev.*, 104:671, 2016.
- Barocas, S., Hardt, M., and Narayanan, A. Fairness in machine learning. *NIPS Tutorial*, 2017.
- Baron, R. M. and Kenny, D. A. The moderator–mediator variable distinction in social psychological research: Conceptual, strategic, and statistical considerations. *Journal of personality and social psychology*, 51(6):1173, 1986.
- Bechavod, Y. and Ligett, K. Learning fair classifiers: A regularization-inspired approach. *arXiv preprint arXiv:1707.00044*, pp. 1733–1782, 2017.
- Bertran, M., Martinez, N., Papadaki, A., Qiu, Q., Rodrigues, M., Reeves, G., and Sapiro, G. Adversarially learned representations for information obfuscation and inference. In Chaudhuri, K. and Salakhutdinov, R. (eds.), *Proceedings of the 36th International Conference on Machine Learning*, volume 97 of *Proceedings of Machine Learning Research*, pp. 614–623, 2019.
- Beutel, A., Chen, J., Zhao, Z., and Chi, E. H. Data decisions and theoretical implications when adversarially learning fair representations, 2017.
- Bousmalis, K., Silberman, N., Dohan, D., Erhan, D., and Krishnan, D. Unsupervised pixel-level domain adaptation with generative adversarial networks. In *Proceedings of the IEEE conference on computer vision and pattern recognition*, pp. 3722–3731, 2017.
- Buolamwini, J. and Gebru, T. Gender shades: Intersectional accuracy disparities in commercial gender classification. In *Conference on fairness, accountability and transparency*, pp. 77–91, 2018.
- Celis, L. E., Deshpande, A., Kathuria, T., and Vishnoi, N. K. How to be fair and diverse? *arXiv preprint arXiv:1610.07183*, 2016.
- Choi, J., Gao, C., Messou, J. C., and Huang, J.-B. Why can’t i dance in the mall? learning to mitigate scene bias in action recognition. In *Advances in Neural Information Processing Systems*, pp. 851–863, 2019.
- Cole, J. H., Underwood, J., Caan, M. W., De Francesco, D., van Zoest, R. A., Leech, R., Wit, F. W., Portegies, P., Geurtsen, G. J., Schmand, B. A., et al. Increased brain-predicted aging in treated HIV disease. *Neurology*, 88(14):1349–1357, 2017.
- Creager, E., Madras, D., Jacobsen, J.-H., Weis, M., Swersky, K., Pitassi, T., and Zemel, R. Flexibly fair representation learning by disentanglement. In Chaudhuri, K. and Salakhutdinov, R. (eds.), *Proceedings of the 36th International Conference on Machine Learning*, volume 97 of *Proceedings of Machine Learning Research*, pp. 1436–1445, Long Beach, California, USA, 09–15 Jun 2019. PMLR.
- Deng, J., Dong, W., Socher, R., Li, L.-J., Li, K., and Fei-Fei, L. Imagenet: A large-scale hierarchical image database. In *2009 IEEE conference on computer vision and pattern recognition*, pp. 248–255. Ieee, 2009.
- Dobrowolska, B., Jkdrzejkiwicz, B., Pilewska-Kozak, A., Zarzycka, D., Ślusarska, B., Deluga, A., Kościółek, A., and Palese, A. Age discrimination in healthcare institutions perceived by seniors and students. *Nursing ethics*, 26(2):443–459, 2019.
- Edwards, H. and Storkey, A. Censoring representations with an adversary. In *ICLR*, 2016.
- Eichler, M., Reisman, A. L., and Borins, E. M. Gender bias in medical research. *Women & Therapy*, 12(4):61–70, 1992.
- Elazar, Y. and Goldberg, Y. Adversarial removal of demographic attributes from text data. In *Proceedings of the 2018 Conference on Empirical Methods in Natural Language Processing*, pp. 11–21, Brussels, Belgium, October–November 2018. Association for Computational Linguistics.
- Esmailzadeh, S., Belivanis, D. I., Pohl, K. M., and Adeli, E. End-to-end alzheimers disease diagnosis and biomarker identification. In *MICCAI-MLMI*, 2018.
- Ganin, Y., Ustinova, E., Ajakan, H., Germain, P., Larochelle, H., Laviolette, F., Marchand, M., and Lempitsky, V. Domain-adversarial training of neural networks. *The Journal of Machine Learning Research*, 17(1):2096–2030, 2016.
- Geitgey, A. Face recognition, 2018. URL [https://pypi.org/project/face\\_recognition/](https://pypi.org/project/face_recognition/).
- Goodfellow, I., Pouget-Abadie, J., Mirza, M., Xu, B., Warde-Farley, D., Ozair, S., Courville, A., and Bengio, Y. Generative adversarial nets. In *NeurIPS*, 2014.

- Hashimoto, T. B., Srivastava, M., Namkoong, H., and Liang, P. Fairness without demographics in repeated loss minimization. In *Proceedings of the International Conference on Machine Learning*, 2018.
- He, K., Zhang, X., Ren, S., and Sun, J. Deep residual learning for image recognition. computer vision and pattern recognition (cvpr). In *2016 IEEE Conference on*, volume 5, pp. 6, 2015.
- Hoffman, J., Tzeng, E., Park, T., Zhu, J.-Y., Isola, P., Saenko, K., Efros, A. A., and Darrell, T. Cycada: Cycle-consistent adversarial domain adaptation. *arXiv preprint arXiv:1711.03213*, 2017.
- Huang, F. and Yates, A. Biased representation learning for domain adaptation. In *Proceedings of the 2012 Joint Conference on Empirical Methods in Natural Language Processing and Computational Natural Language Learning*, pp. 1313–1323. Association for Computational Linguistics, 2012.
- Khademi, A. and Honavar, V. Algorithmic bias in recidivism prediction: A causal perspective. In *AAAI*, 2020.
- Khosla, A., Zhou, T., Malisiewicz, T., Efros, A. A., and Torralba, A. Undoing the damage of dataset bias. In *European Conference on Computer Vision*, pp. 158–171. Springer, 2012.
- Khullar, D. A.I. could worsen health disparities, 2019. URL <https://www.nytimes.com/2019/01/31/opinion/ai-bias-healthcare.html>.
- Kim, B., Kim, H., Kim, K., Kim, S., and Kim, J. Learning not to learn: Training deep neural networks with biased data. In *Proceedings of the IEEE Conference on Computer Vision and Pattern Recognition*, pp. 9012–9020, 2019.
- Lee, N. T., Resnick, P., and Barton, G. Algorithmic bias detection and mitigation: Best practices and policies to reduce consumer harms. *Center for Technology Innovation, Brookings*. Tillgänglig online: <https://www.brookings.edu/research/algorithmic-bias-detection-and-mitigation-bestpractices-and-policies-to-reduce-consumer-harms/#footnote-7> (2019-10-01), 2019.
- Li, Y. and Vasconcelos, N. REPAIR: Removing representation bias by dataset resampling. In *Proceedings of the IEEE Conference on Computer Vision and Pattern Recognition*, pp. 9572–9581, 2019.
- Liu, L. T., Dean, S., Rolf, E., Simchowitz, M., and Hardt, M. Delayed impact of fair machine learning. In *Proceedings of the International Conference on Machine Learning*, 2018.
- Lu, Y., Kumar, A., Zhai, S., Cheng, Y., Javidi, T., and Feris, R. Fully-adaptive feature sharing in multi-task networks with applications in person attribute classification. In *Proceedings of the IEEE Conference on Computer Vision and Pattern Recognition*, pp. 5334–5343, 2017.
- Maaten, L. v. d. and Hinton, G. Visualizing data using t-SNE. *JMLR*, 9, 2008.
- Miller, C. Algorithms and bias, 2015. URL <https://www.nytimes.com/2015/08/11/upshot/algorithms-and-bias-q-and-a-with-cynthia-dwork.html>.
- Moyer, D., Gao, S., Brekelmans, R., Galstyan, A., and Ver Steeg, G. Invariant representations without adversarial training. In Bengio, S., Wallach, H., Larochelle, H., Grauman, K., Cesa-Bianchi, N., and Garnett, R. (eds.), *Advances in Neural Information Processing Systems 31*, pp. 9084–9093. 2018.
- Nie, D., Zhang, H., Adeli, E., Liu, L., and Shen, D. 3d deep learning for multi-modal imaging-guided survival time prediction of brain tumor patients. In *International Conference on Medical Image Computing and Computer-Assisted Intervention*, pp. 212–220. Springer, 2016.
- Pourhoseingholi, M. A., Baghestani, A. R., and Vahedi, M. How to control confounding effects by statistical analysis. *Gastroenterol Hepatol Bed Bench*, 5(2):79, 2012.
- Ranzato, M., Huang, F. J., Boureau, Y.-L., and LeCun, Y. Unsupervised learning of invariant feature hierarchies with applications to object recognition. In *2007 IEEE conference on computer vision and pattern recognition*, pp. 1–8. IEEE, 2007.
- Rao, A. et al. Predictive modelling using neuroimaging data in the presence of confounds. *NeuroImage*, 150:23–49, 2017.
- Roy, P. C. and Boddeti, V. N. Mitigating information leakage in image representations: A maximum entropy approach. *CoRR*, abs/1904.05514, 2019. URL <http://arxiv.org/abs/1904.05514>.
- Sadeghi, B., Yu, R., and Boddeti, V. On the global optima of kernelized adversarial representation learning. In *Proceedings of the IEEE International Conference on Computer Vision*, pp. 7971–7979, 2019.
- Salimi, B., Rodriguez, L., Howe, B., and Suci, D. Interventional fairness: Causal database repair for algorithmic fairness. In *Proceedings of the 2019 International Conference on Management of Data*, pp. 793–810, 2019.
- Simonyan, K. and Zisserman, A. Very deep convolutional networks for large-scale image recognition. In *ICLR*, 2015.

- Simonyan, K., Vedaldi, A., and Zisserman, A. Deep inside convolutional networks: Visualising image classification models and saliency maps. In *ICLR*, 2014.
- Song, J., Kalluri, P., Grover, A., Zhao, S., and Ermon, S. Learning controllable fair representations. In Chaudhuri, K. and Sugiyama, M. (eds.), *Proceedings of Machine Learning Research*, volume 89 of *Proceedings of Machine Learning Research*, pp. 2164–2173. PMLR, 2019.
- Springenberg, J. T. Unsupervised and semi-supervised learning with categorical generative adversarial networks. *arXiv preprint arXiv:1511.06390*, 2015.
- Székely, G. J., Rizzo, M. L., Bakirov, N. K., et al. Measuring and testing dependence by correlation of distances. *The annals of statistics*, 35(6):2769–2794, 2007.
- Tommasi, T., Patricia, N., Caputo, B., and Tuytelaars, T. A deeper look at dataset bias. In *Domain adaptation in computer vision applications*, pp. 37–55. Springer, 2017.
- Tzeng, E., Hoffman, J., Saenko, K., and Darrell, T. Adversarial discriminative domain adaptation. In *Proceedings of the IEEE Conference on Computer Vision and Pattern Recognition*, pp. 7167–7176, 2017.
- Wang, T., Zhao, J., Yatskar, M., Chang, K.-W., and Ordonez, V. Balanced datasets are not enough: Estimating and mitigating gender bias in deep image representations. In *Proceedings of the IEEE International Conference on Computer Vision*, pp. 5310–5319, 2019.
- Weinzaepfel, P. and Rogez, G. Mimetics: Towards understanding human actions out of context. *arXiv preprint arXiv:1912.07249*, 2019.
- Wooldridge, J. M. *Econometric Analysis of Cross Section and Panel Data (2nd ed.)*. The MIT Press, London, 2010.
- Xie, Q., Dai, Z., Du, Y., Hovy, E., and Neubig, G. Controllable invariance through adversarial feature learning. In *Advances in Neural Information Processing Systems*, pp. 585–596, 2017.
- Yang, K., Qinami, K., Fei-Fei, L., Deng, J., and Russakovsky, O. Towards fairer datasets: Filtering and balancing the distribution of the people subtree in the imagenet hierarchy. *Image-Net*, 2019.
- Zafar, M. B., Valera, I., Rodriguez, M. G., and Gummadi, K. P. Fairness Constraints: Mechanisms for Fair Classification. In Singh, A. and Zhu, J. (eds.), *Proceedings of the 20th International Conference on Artificial Intelligence and Statistics*, volume 54 of *Proceedings of Machine Learning Research*, pp. 962–970. PMLR, 2017.
- Zemel, R., Wu, Y., Swersky, K., Pitassi, T., and Dwork, C. Learning fair representations. In *International Conference on Machine Learning*, pp. 325–333, 2013.
- Zhang, B. H., Lemoine, B., and Mitchell, M. Mitigating unwanted biases with adversarial learning. In *Proceedings of the 2018 AAAI/ACM Conference on AI, Ethics, and Society*, pp. 335–340. ACM, 2018.